Journal of Oceanology and Limnology
Vol. 38 No. 3, P. 619-633, 2020
https://doi.org/10.1007/s00343-019-8365-9

Comparison of sedimentary organic carbon loading in the Yap Trench and other marine environments*

LI Dong[1], ZHAO Jun[1, **], LIU Chenggang[1], SUN Chengjun[2], CHEN Jianfang[1], PAN Jianming[1], HAN Zhengbing[1], HU Ji[1]

[1] *Key Laboratory of Marine Ecosystem and Biogeochemistry*, *State Oceanic Administration*, *Second Institute of Oceanography*, *Ministry of Natural Resources*, *Hangzhou 310012*, *China*

[2] *Key Laboratory of Marine Eco-environmental Science and Technology*, *Marine Bioresource and Environment Research Center*, *First Institute of Oceanography*, *Ministry of Natural Resources*, *Qingdao 266061*, *China*

Received Dec. 18, 2018; accepted in principle Apr. 25, 2019; accepted for publication Jul. 10, 2019

Abstract Knowledge about organic carbon loadings (ratio of sedimentary organic carbon (SOC) content to specific surface area (SSA)) and the fate of organic carbon (OC) is critical to understand the marine carbon cycle. We investigated the variations in the patterns of OC loadings and the preservation capacities of sedimentary OC in the Yap Trench and other marine environments. The average OC loading in sediment cores from various marine environments decreases with increasing water depth at a rate of ~0.06 mg OC/(m^2·km) (R^2=0.23, P<0.01). Distinct low OC loadings (0.09±0.04 mg OC/m^2) were observed in the Yap Trench, with the lowest values as ~0.02 mg OC/m^2. A further comparative analysis indicated that OC/SSA=0.2 mg OC/m^2 is a good indicator to distinguish between oxic deep-sea regions and suboxic energetic deltaic areas. Regression analysis between OC loading and bulk carbon isotope compositions indicates that marine OC ($\delta^{13}C$ ~-20.4‰ to -18.6‰) dominates the lost OC within the Yap Trench and does not differ from that of the abyssal zone. In contrast, terrestrial OC with $\delta^{13}C$ values of approximately -27.4‰ to -20.5‰ was the major source of remineralized OC in the sublittoral zone. The ratios of OC loadings in the bottom layer relative to those in the top layers of sediment cores indicate that the preservation capacities of hadal trenches are much lower than those of other environments, and only approximately 30% of the SOC deposited in hadal trenches is finally buried. The value is equivalent to 0.066% of the primary production-derived OC and much lower than the global ocean average (~0.3%). Overall, the hadal zone exhibits the lowest OC loading and preservation capacity of SOC of the different marine environments investigated, despite the occurrence of a notable funneling effect.

Keyword: Yap Trench; hadal zone; organic carbon loading; specific surface area; preservation capacity

1 INTRODUCTION

Typical hadal zones (water depth >6 000 m) are found in deep ocean trenches formed by the convergent movements of two oceanic lithospheric plates at subduction zones (Fig.1a) (Clift and Vannucchi, 2004). While limited biogeochemical studies have been done, the particular geological structures and physiognomic characteristics of hadal trenches may lead this unique environment to play a key role in the global organic carbon cycle, as the funnel-like shape of a hadal trench easily traps settling particulate matter delivered from natural sedimentation, ocean circulation and submarine turbidity currents and serves as a large-scale sediment trap in the deep ocean (Longhurst et al., 1995; Danovaro et al., 2003; Glud et al., 2013; Li et al., 2018). Widespread bare rock and steep slopes in hadal trenches significantly weaken the velocity of water flow (~cm/s) (Fig.1a) (Hallock and Teague, 1996; Fujio et al., 2000; Taira et al., 2004), and it is difficult for deposits to be physically moved out of the hadal trench. In the active convergent

* Supported by the National Natural Science Foundation of China (No. 41606090), the National Key Basic Research and Development Project of China (No. 2015CB755904), and the Scientific Research Fund of the Second Institute of Oceanography (MNR) (Nos. JG1624, JG1516)
** Corresponding author: jzhao@sio.org.cn

plate boundary system that forms a hadal trench, sediment remobilization induced by earthquakes and associated turbidity currents triggers the formation of dense nepheloid layers resulting in high deposition rates and sedimentary organic carbon (SOC) contents (Fig.1a) (Nozaki and Ohta, 1993; Bao et al., 2018). Moreover, subduction of the oceanic plate into the hot mantle promotes delivery of the overlying SOC to the deep earth interior, such that hadal trenches serve as an organic carbon sink in the deep ocean (Fig.1a) (Danovaro et al., 2003; Glud et al., 2013; Nunoura et al., 2015).

Acting as a global sink for excess carbon dioxide in the atmosphere, the oceans fix atmospheric CO_2 via the so-called "biological pump", whereby particulate organic matter sinks and is buried in the deep ocean (Lasaga et al., 1985). Exploring the final fate of settling OC is crucial for evaluating the strength of atmospheric CO_2 fixation by the ocean, which dominates the negative feedback loop associated with global warming and thus regulates the global carbon cycle (Mayer, 1994a; Chen et al., 2004, 2015; Blair and Aller, 2012). On geologic timescales, the preservation capacity of SOC in marine environments relies heavily on the OC loading of settling particulate matter (Mayer, 1995; Keil et al., 1997a; Blair and Aller, 2012; Li et al., 2017). The ratio of OC content to the specific surface area (OC/SSA) of the sediment has been widely used to trace variations of sedimentary OC loading in different marine environments (Mayer, 1994b; Aller et al., 2008; Goñi et al., 2013; Li et al., 2014). Specific ranges of OC loadings in sedimentary deposits have been used to distinguish preservation status and characterize marine settings as reflecting a net balance between loss and supply of SOC under distinct environmental regions (Aller et al., 2010; Zonneveld et al., 2010; Blair and Aller, 2012; Li et al., 2014; Yao et al., 2014). For example, significantly lower OC loadings associated with mobile mud belts in continental marginal seas indicate efficient remineralization of SOC in this environment (Aller, 1998; Aller and Blair, 2004, 2006; Yao et al., 2014). In conjunction with previous research, research presented here investigating the features of OC loadings in the extreme and least-studied hadal environments that act as potential sediment traps and carbon sinks in the deep ocean provides more comprehensive information on the marine organic carbon cycle.

The Yap Trench is located in the equatorial western Pacific Ocean at the junction between the oceanic Pacific Plate, the Philippine Plate and the Caroline Plate constituting a link between the Philippine Trench and Mariana Trench. The primary production rate of the overlying euphotic layer is ~82 g OC/(m^2·a), which is comparable to that of the adjacent Mariana Trench (Longhurst et al., 1995; Lutz et al., 2007; Jamieson, 2015). Trace element ratios (Ni/Co and V/Cr) in sediments from the Yap Trench indicate an oxic sedimentary environment, which is overlain by dissolved oxygen (DO)-enriched local bottom water (approximately 5.1 mg/L) (Li et al., 2018; Yue et al., 2018). To accurately determine variations in the OC loading of the sediments and evaluate possible factors influencing OC loading within the Yap Trench and adjacent abyssal plain, push core sediments were collected from the northern and southern Yap Trench and box core sediments were collected from the adjacent abyssal plain. The SSA, OC content, and $\delta^{13}C$ values of core sediments were analyzed. Spatial and vertical variations in SOC loading and preservation status in different regions of the Yap Trench and the adjacent abyssal plain were then calculated. Literature values on OC loadings of sediments obtained from shallower marine environments (including continental marginal sea, slope, ocean basin, and abyssal plain) were also compiled for comparative analysis. This work extends our knowledge about the patterns of OC loading in the ocean and contributes to a better understanding of the role that hadal trenches play in marine organic carbon cycles.

2 SAMPLE COLLECTION AND ANALYSIS

Six push cores were collected using China's first manned deep sea bathyscaphe, *Jiaolong*, and additionally, one box core was collected during the cruises of the 37th and 38th *China Oceanic* Expeditions of Spring 2016 and Spring 2017 onboard the R/V *Xiangyanghong 09*. Detailed sampling information is shown in Table 1 and Fig.1c. These sediment cores cover the northern and southern Yap Trench, including both walls of the hadal trench as well as the adjacent abyssal area on the Caroline Plate. These cores were sliced at 1 cm intervals, and subsamples were placed in plastic bags and stored at -20°C. In the lab, each sample was freeze-dried; a subsample was ground to ensure sample homogeneity for OC% and ^{13}C analyses, and the remaining unground subsamples were prepared for SSA analysis.

Homogenized and precisely weighed dry sediments were placed into a silver capsule, after which inorganic carbon was removed by exposure to hydrochloric acid vapor for 24 h at room temperature.

Table 1 Sampling site information, OC contents, carbon stable isotopes, specific surface areas (SSA) and OC loadings of core sediments from the Yap Trench and adjacent abyssal regions

Site / style	Water depth / Core length / Location	Longitude (°E)	Latitude (°N)	OC (%)		$\delta^{13}C$ (‰)		SSA (m^2/g)		OC/SSA (mg OC/m^2)	
				Range	Mean±sd	Range	Mean±sd	Range	Mean±sd	Range	Mean±sd
DIVE109/ Push core	4 435 m / 19 cm / Landward slope of northern Yap Trench	138.39	9.90	0.07–0.26	0.15±0.07 (*n*=19)	-21.53–-19.52	-20.29±0.47 (*n*=19)	10.92–20.96	15.54±2.51 (*n*=19)	0.04–0.14	0.10±0.03 (*n*=19)
DIVE111/ Push core	6 775 m / 7 cm / Landward slope of northern Yap Trench	138.51	9.86	0.08–0.64	0.19±0.19 (*n*=7)	-22.7–-20.2	-21.27±0.81 (*n*=7)	17.10–51.29	36.86±11.09 (*n*=7)	0.02–0.14	0.05±0.04 (*n*=7)
DIVE113/ Push core	6 574 m / 25 cm / Seaward slope of northern Yap Trench	138.65	9.87	0.13–0.39	0.27±0.08 (*n*=25)	-21.76–-18.92	-19.93±0.63 (*n*=25)	29.85–47.54	37.26±4.80 (*n*=25)	0.04–0.12	0.07±0.02 (*n*=25)
DIVE149/ Push core	4 993 m / 14 cm / Landward slope of southern Yap Trench	137.55	8.06	0.14–0.76	0.38±0.18 (*n*=14)	-22.48–-19.55	-20.78±0.85 (*n*=14)	16.36–44.47	31.61±9.11 (*n*=14)	0.08–0.22	0.12±0.04 (*n*=14)
DIVE151/ Push core	6 582 m / 21 cm / Landward slope of southern Yap Trench	137.63	8.04	0.21–0.48	0.31±0.08 (*n*=21)	-21.80–-20.04	-20.74±0.60 (*n*=21)	30.50–47.51	41.60±4.19 (*n*=21)	0.04–0.10	0.07±0.02 (*n*=21)
DIVE152/ Push core	6 681 m / 18 cm / Seaward slope of southern Yap Trench	137.84	8.02	0.28–0.52	0.39±0.07 (*n*=18)	-21.41–-20.08	-20.83±0.51 (*n*=18)	17.52–47.90	42.04±7.68 (*n*=18)	0.06–0.30	0.10±0.06 (*n*=18)
S01/ Multi-tube	5 389 m / 12 cm / Abyssal region east of Yap Trench	138.70	9.66	0.22–0.40	0.29±0.05 (*n*=12)	-22.82–-20.75	-21.30±0.75 (*n*=12)	11.64–21.76	17.26±2.99 (*n*=12)	0.14–0.21	0.17±0.02 (*n*=12)

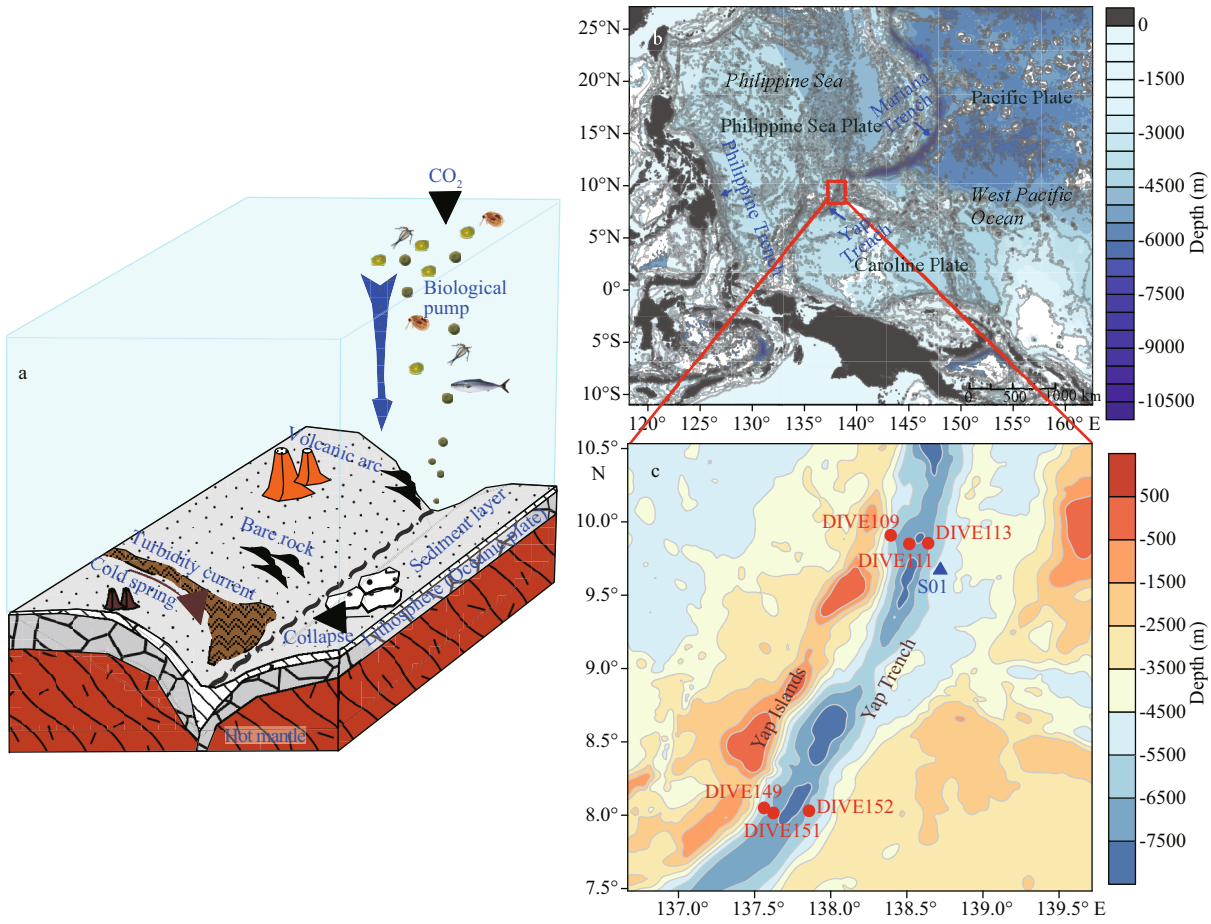

Fig.1 Conceptual model of trench geography and habitat characteristics (a) and sampling sites in the Yap Trench and adjacent abyssal region (b and c)

Fujiwara et al., 2000; Jamieson and Fujii, 2011; Ichino et al., 2015; Jamieson, 2015.

Dried carbonate-free samples were then transferred into a tin capsule and analyzed on a Flash EA 1112 HT nitrogen/carbon analyzer (Thermo Electron SPA, USA) interfaced with a DELTA V *Advantage* continuous flow isotope ratio mass spectrometer (Thermo Finnigan Instruments, USA). Replicate analyses of samples yield a relative standard deviation of less than 0.8% for OC%. The $\delta^{13}C$ was expressed in δ notation per mil relative to the international standard Vienna Pee Dee belemnite. The precision of $\delta^{13}C$ analyses was better than ±0.2‰ based on replicate analyses.

The SSA values of sediments were determined by the Multi-point Brunauer-Emmett-Teller method (with N_2 as adsorbent and five adsorption isotherm points) using an automatic surface analyzer (3H-2000PS1, Beishide Instrument Technology (Beijing) Co. Ltd., China). Unground dry sediments were combusted at 350°C for 12 h to remove organic matter and water prior to instrumental analysis, a pretreatment method has proven to be effective for removing OC and is widely used in analyzing marine sediments (Keil et al., 1997b; Aller and Blair, 2006; Yao et al., 2014; Li et al., 2017). To further remove volatile matter, the organic matter-free sediment samples were then degassed at 300°C under vacuum conditions for 1 h. The accuracy of SSA measurements was assessed based on analysis of a standard material (mesoporous SiO_2) provided by Beishide Company (Beijing, China). Replicate analyses indicated that the relative standard deviation was less than 5%.

Additionally, data on the OC%, SSA, and OC loading of surface and core sediments collected from other marine environments (in addition to the hadal zone (>6 000 m)) were compiled from the scientific literature (Supplementary Table S1). Data reported in different units were recalculated and normalized. To obtain the final asymptotic values of OC loadings, different lengths of sediment cores were considered in different marine environments, with longer core lengths considered in continental marginal seas and shorter core lengths considered in deep-sea sites (Supplementary Table S1). These available data were divided into four groups according to sampling depth, including the sublittoral region with water depth <300 m, the bathyal zone with water depth between 300 m and 3 500 m, and the abyssal zone with water depth ranging from 3 500 m to 6 000 m. Details on the sampling locations for both the literature data and those used in this study are specified in the captions and legends of each figure.

The approximate preservation capacity of SOC in sediment cores was calculated using the following equation: $\%OC_{preservation}=OC/SSA_{lower\ layer}/OC/SSA_{upper\ layer}$. In this equation, the $OC/SSA_{lower\ layer}$ is set equal to the minimum OC loading of the bottom 3 layers, which is assumed to represent the final asymptotic value of OC loading in the sediment core, and the $OC/SSA_{upper\ layer}$ is set equal to the maximum OC loading of the top 3 layers which is assumed to represent the initial value of OC loading in the sediment core. Although this calculation method introduces some uncertainty because of differences in time scales between different sediment cores, we can roughly evaluate the potential and ultimate preservation capacity of SOC in specific marine environments by comparing the asymptotic value at the bottom of the sediment core with the maximum value at the top of the core. This preservation capacity can be taken to represent the percentage of SOC that is ultimately buried relative to the initially deposited SOC, following a sufficiently long post-depositional degradation process (Blair and Aller, 2012).

Statistical analyses (Pearson's correlation and significance testing) were performed using the SPSS20 software. The sampling map was constructed using Surfer13 software, and other figures were drawn using Origin2017 software.

3 RESULT

Variations in the ranges and average values of OC%, $\delta^{13}C$, SSA and OC loading for each of the measured sediment cores are shown in Table 1, Figs.2 and 3. In general, values for the OC%, $\delta^{13}C$, SSA and OC loading of the studied cores reveal remarkable regional differences within the study region; results of significance testing are shown in Supplementary Table S2.

The vertical OC% profiles obtained from sediment cores exhibit a decreasing trend with depth (Fig.2). Furthermore, the average OC% in sediment cores from the southern Yap Trench is higher than those from the northern trench ($P<0.01$) (Fig.2a, Supplementary Table S2). The $\delta^{13}C$ values display no significant difference between the two sides of the trench slope ($P>0.05$, except for the DIVE111 site), but a significant difference between the southern and northern trench ($P<0.05$, except for the DIVE111 site) (Supplementary Table S2). Lower $\delta^{13}C$ values are usually found in sediment layers at the bottom of the cores (in addition to core DIVE113) (Fig.2b).

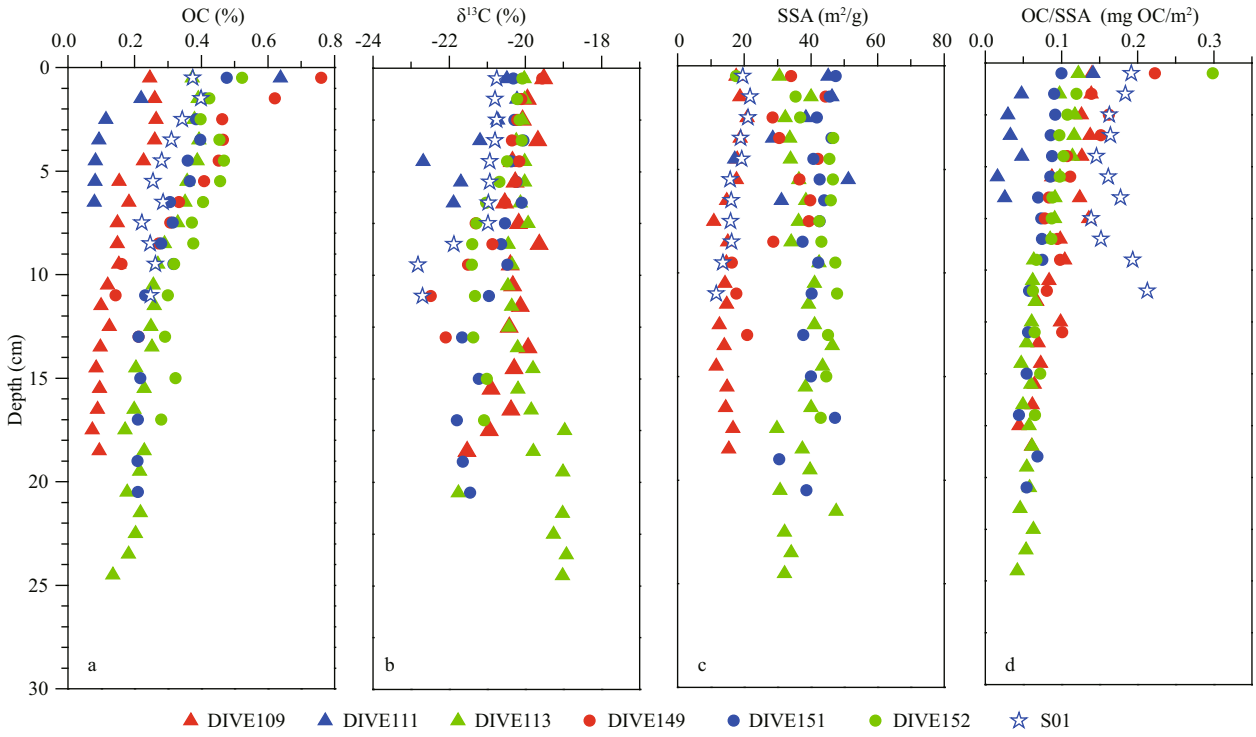

Fig.2 Vertical profiles of OC (a), $\delta^{13}C$ (b), SSA (c) and OC (d) loading values of seven sediment cores collected from the Yap Trench and adjacent abyssal region

Red, blue and green triangles represent sites DIVE109, DIVE111 and DIVE113 in the northern Yap Trench, respectively; red, blue and green circles represent sites DIVE149, DIVE151 and DIVE152 in the southern Yap Trench; blue pentagrams represent Site S01 in the abyssal region east of the Yap Trench.

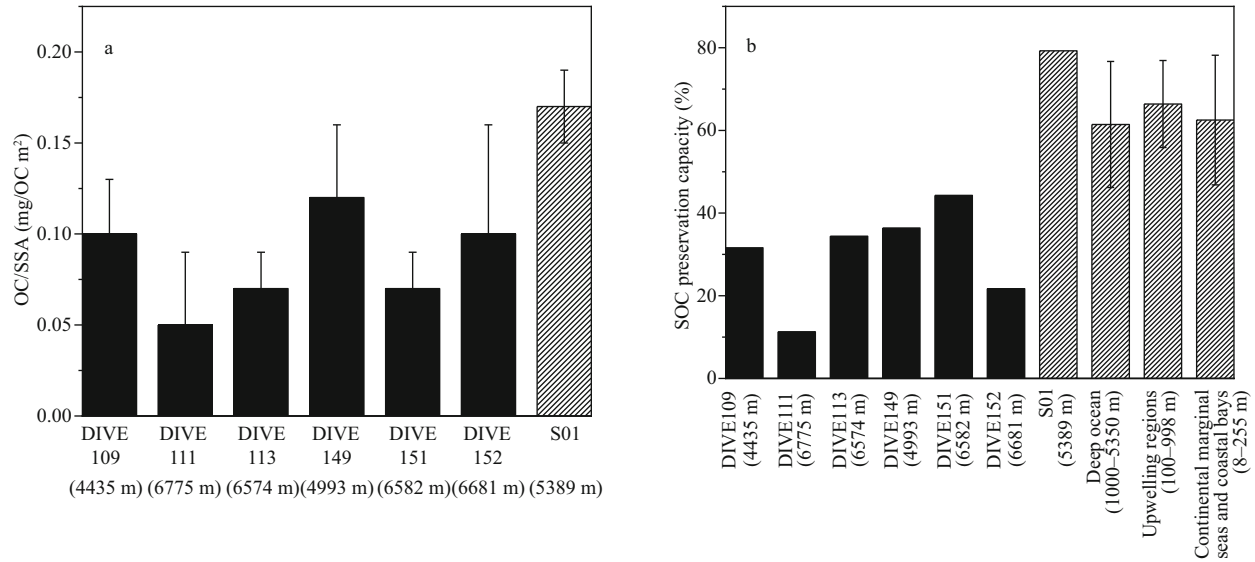

Fig.3 Average OC loadings of sediment cores in this study (a) and comparison of OC preservation capacities in the Yap Trench and those reported for other marine environments (b)

Black bars represent the standard deviation. Deep oceans include the NE Pacific slope, the NW Atlantic slope, and central Indian Ocean. Upwelling regions include the California slope and the Peru slope. Continental marginal seas and coastal bays include the Siberian Sea, the Beaufort Sea, the Chukchi Sea, the East China Sea, the Gulf of Papua, the Amazon Estuary, the Mississippi Estuary, the Chesapeake Bay, and the Gulf of Maine (unpublished data of East China Sea core sediments; Mayer, 1994a, b; Aller and Blair, 2006; Aller et al., 2008; Nath et al., 2012; Goñi et al., 2013; Vonk et al., 2015; Bröder et al., 2016).

In evaluating the physical structure of sedimentary particles, SSA values exhibit significant differences between the two trench slopes and between the southern and northern regions (P<0.05), with higher

average values found in the southern region and on the seaward trench slopes (Fig.2c, Supplementary Table S2). Additionally, the SSA values in the Yap Trench can be divided into two types. The first type consisted of sites located in shallower abyssal water (i.e. DIVE109 and S01), which exhibit lower SSA values and a smaller ranges of differences in SSA between sites; the second type, located in deeper hadal regions (e.g., cores DIVE111 and DIVE151), exhibit higher SSA values and a wider variation in the ranges of SSA among sites (Fig.4).

With respect to the OC loading value, most sediment cores exhibited a downward decreasing vertical trend with the exception of core S01, where OC loading increases significantly below a depth of 7 cm (Fig.2d) and higher OC loadings in shallower sediment cores (P<0.05, Supplementary Table S2, Fig.3a). For example, cores collected from sampling locations on the shallower landward trench slope (e.g., DIVE109 and 149) had the highest OC loadings, despite having the smallest sediment SSA ratios (Fig.3a). The OC loadings in cores located on the deep distal side of the Yap Trench ranked second highest, and sites in the deeper landward trench wall had the lowest OC/SSA ratios (Fig.3a). In core S01, which was located in the abyssal region east of the Yap Trench, the average OC% and $\delta^{13}C$ values were moderate compared with those in the Yap Trench, and significantly lower SSA and the highest OC loading were observed in these cores (P<0.01, Fig.2, Supplementary Table S2).

Regional disparities in the linear relationships between sedimentary OC% and SSA were observed in the Yap Trench. As shown in Fig.4, positive correlations between OC% and SSA are observed for sites DIVE109 (R=0.71, P<0.01, n=19), DIVE149 (R=0.64, P<0.05, n=12) and DIVE151 (R=0.62, P<0.05, n=16), all of which are located on the landward side of the Yap Trench (Fig.4). In contrast, weak negative linear relationships between OC content and SSA values were found for site DIVE152 (R=-0.53, P=0.05, n=14) located on the distal side of the Yap Trench (Fig.4). Correlations of OC% and OC loadings with $\delta^{13}C$ values were also calculated. Significant positive relationships between OC% and $\delta^{13}C$ values are found in sites DIVE109 (R=0.58, P=0.01, n=19), DIVE149 (R=0.89, P<0.01, n=12), DIVE151 (R=0.86, P<0.01, n=16), and DIVE152 (R=0.77, P<0.01, n=14), while no correlation occurrs in sites DIVE111, DIVE113 and S01 (P>0.05). A similar correlation between OC loadings and $\delta^{13}C$ values at the study sites is also observed. Significant positive linear relationships occurr in all southern Yap Trench sites (DIVE149: R=0.69, P<0.05, n=12; DIVE151: R=0.82, P<0.01, n=16; DIVE152: R=0.61, P<0.05, n=14) and site DIVE109 (R=0.61, P<0.01, n=19); no correlation is observed in sites DIVE111, DIVE113 and S01 (P>0.05).

The calculated preservation capacities of SOC under different marine regimes are shown in Fig.3b. In general, the percentage of SOC ultimately preserved is 62%±16% in continental marginal seas and coastal bays (n=15), 66%±11% in upwelling slope regions (n=4), and 61%±15% in normal deep oceans (n=5) (Fig.3b). Within the Yap Trench, the calculated preservation capacity is approximately 11%–44%, with an average value of approximately 30%±11% (n=6). Site S01 exhibits a relatively high value (82%). In addition, stronger SOC preservation capacity is observed in the southern Yap Trench compared with the northern trench, and the lowest and highest preservation efficiencies occur in the DIVE111 and DIVE151 sites, respectively (Fig.3b). For the most part, SOC preservation capacity in the Yap Trench is remarkably lower than that of average marine environments (P<0.01, Fig.3b).

4 DISCUSSION

4.1 OC loading variations under different marine regimes

The index of OC/SSA ratios in sediments has been successfully applied in various marine environments (e.g., estuaries, shelf regions, slopes, abyssal plains and basins) to trace the influences of physical, chemical and biological processes on the OC loading capacity of marine sediments (Mayer, 1994b; Aller and Blair, 2004; Aller et al., 2008; Blair and Aller, 2012; Li et al., 2017). In this study, remarkable regional variations in OC/SSA ratios within the Yap Trench and among different marine regimes (Figs.3 & 6) and the corresponding shifts in OC% and SSA values (Figs.4 & 5) suggest that multiple factors are important in determining OC loading capacity from shallow coastal areas to deep oceans.

The increased length of oxygen exposure time with increasing water depth during the pre-depositional degradation process has the most important effect on the OC loading of sediments in different marine environments. As shown in Figs.3 & 6, whether in hadal trenches or other marine environments, average OC loadings in sediment cores decrease significantly

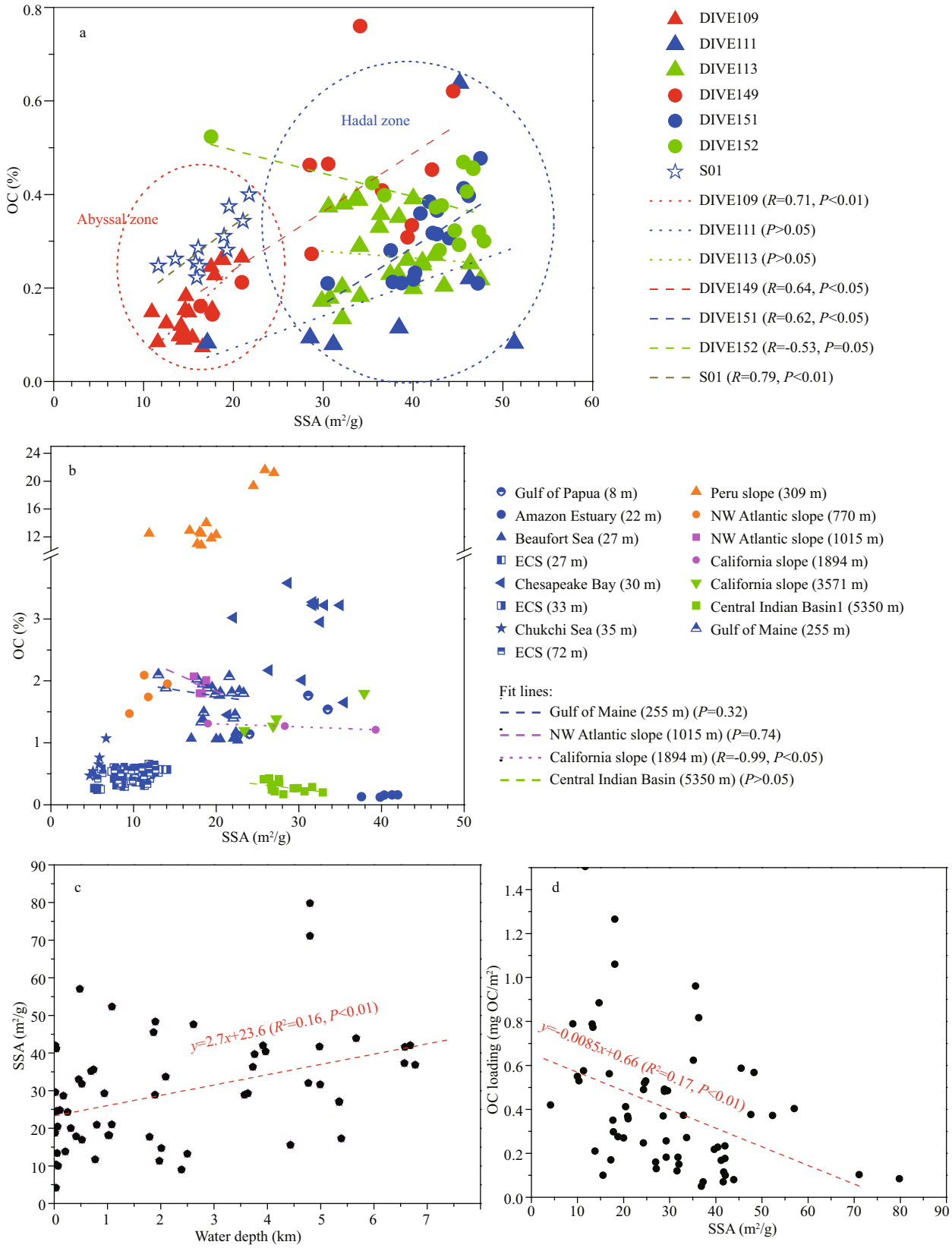

Fig.4 Correlations between SSA and OC% of core sediments from the Yap Trench and adjacent abyssal region (a); other marine environments (b); average SSA versus water depth (c); OC loading versus SSA in distinct marine environments (d)

The dotted red lines are the regression lines. In (b), only fit lines of non-positive relationships of sediment cores are shown (Mayer, 1994a, b; Aller and Blair 2006; Aller et al., 2008; Nath et al., 2012; Goñi et al., 2013; Li et al., 2017).

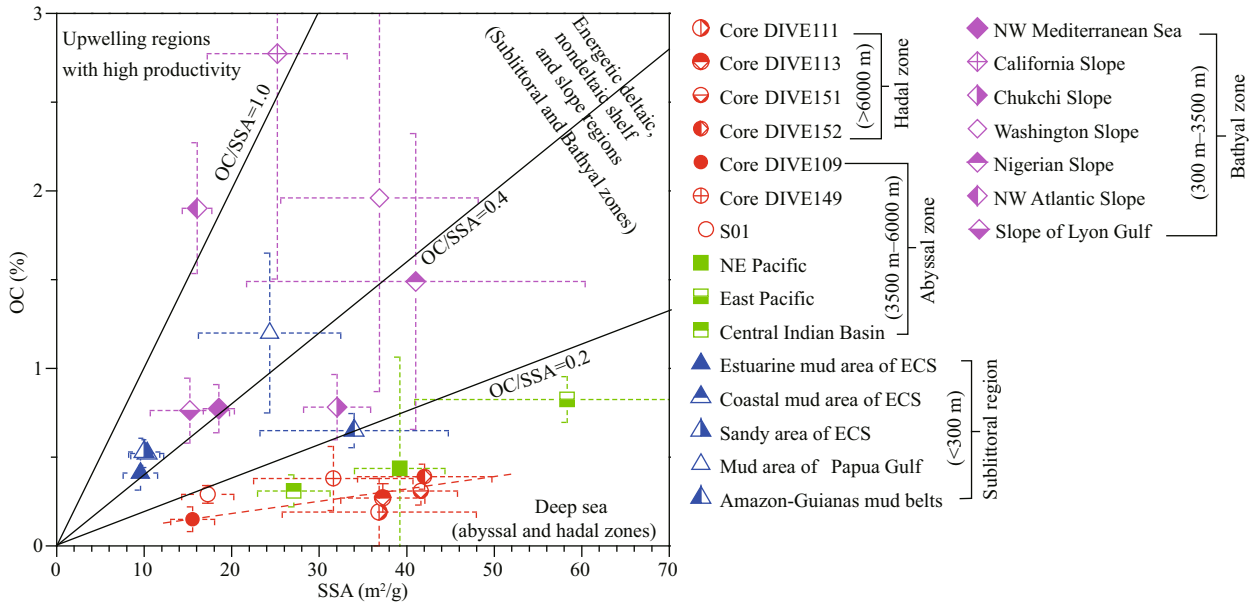

Fig.5 Variations in average OC% and SSA of core sediments from different marine environments

ECS: East China Sea. The black lines are reference lines following different OC/SSA ratios, and the error bars are the standard deviations of the OC% and SSA values in different sediment cores. The red dotted line is the regression line for core samples from the Yap Trench (y=0.007x+0.034, R^2=0.70, P<0.01) (unpublished data of East China Sea core sediments; Mayer, 1994a, b; Aller and Blair, 2006; Aller et al., 2008; Nath et al., 2012; Yao et al., 2014; Vonk et al., 2015).

with increasing water depth, and the lowest OC loadings in marine sediments are found in hadal trenches. Efficient heterotrophic microorganism decomposition of POC attached to settling particulate matter may be responsible for these declining OC/SSA ratios, as suggested by the decrease in the organic matter flux of settling particulate with increasing water depth and retention time in the water column (Mayer, 1994a; Longhurst et al., 1995; Lutz et al., 2007; Honjo et al., 2008). Thus, biogeochemical processes that could increase the POC settling flux or reduce oxygen exposure time during the settling process would significantly increase OC loadings. In this study, within the Yap Trench, although water depths were similar between sediment cores collected in the southern (DIVE151 and DIVE152) and northern (DIVE111 and DIVE113) Yap Trench, significantly higher OC% and OC loadings were observed in the southern region of the Yap Trench (Fig.4 and Table 1). We suggest that the difference in primary production of the overlying euphotic layer, as demonstrated by remarkably higher average chlorophyll-*a* concentrations in euphotic layers (0–200 m) of the southern Yap Trench (~59.4 ng/L) compared with the northern Yap Trench (13.6 ng/L) (unpublished data), is a likely reason for distinct OC% and OC loadings in the southern and northern Yap Trench. Moreover, characteristic loading ratios have been used to differentiate between different environmental regions,

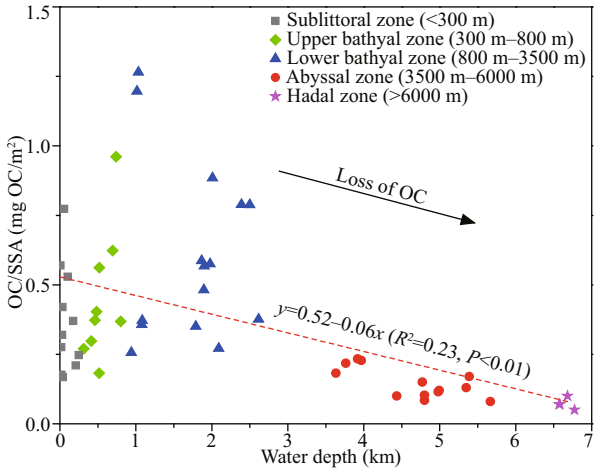

Fig.6 OC loadings of core sediments vs. sampling water depth for samples collected from distinct marine environments

The dotted lines represent the roughly calculated linear fits of rate of decrease in OC loading with increasing water depth. The sublittoral zone includes the Gulf of Papua, the Amazon-Guiana mud belt, the ECS inner shelf, the Chukchi shelf, the Mackenzie shelf, the Chukchi slope, the Nigerian slope and the Washington slope; the upper bathyal zone includes the Washington slope, the Gulf of Lyon, the Mackenzie shelf, the Nigerian slope, the Chukchi slope, the NW Mediterranean Sea, the Skagerrak Strait, the Washington slope and the Gulf of Lyon; the lower bathyal zone includes the Chukchi slope, the NW Atlantic slope, the NW Mediterranean Sea, the Nigerian slope, the Washington slope, the California slope and the Gulf of Lyon; the abyssal zone includes the Yap Trench slope and adjacent plain, the Chukchi slope, the east Pacific Ocean, the NE Pacific Ocean and the central Indian Basin; and the hadal zone includes the Yap Trench (unpublished data of East China Sea core sediments; Mayer, 1994a, b; Aller and Blair, 2006; Aller et al., 2008; Nath et al., 2012; Yao et al., 2014; Vonk et al., 2015; Li et al., 2017).

with >1.0 mg OC/m^2 being used in upwelling regions, 0.4–1.0 mg OC/m^2 in non-deltaic shelf regions and <0.4 mg OC/m^2 for energetic deltaic sediments (Fig.5). In this study, we found that almost all abyssal and hadal samples had loading ratios <0.2 mg OC/m^2, which suggests that this loading ratio is a good indicator to distinguish the oxic deep-sea region from suboxic energetic deltaic area (Fig.5). Using a simple linear fitting method, we calculated that the reduction rate in sedimentary OC loading with increasing water depth is approximately 0.06 mg OC/(m^2·km) (Fig.6). The lowest OC loading may be kept constant at approximately 0.02 mg OC/m^2 (the lowest value in Yap Trench samples) due to constant OC% in the bottom of the hadal trench (>7 000 m) (Luo et al., 2017).

Post-depositional processes, especially reworking in hydrodynamic environments and in situ oxidation reactions at the sediment-water interface, would also decrease OC loadings. Due to the severity of sediment resuspension and active oxidation of SOC (Aller, 1998; Aller and Blair, 2004, 2006; Yao et al., 2014), even with shallow water depths and relatively high POC deposition fluxes in the neritic zone (e.g., East China Sea inner shelf: ~468±262 mg OC/(m^2·d); Amazon River plume: ~1 867±768 mg OC/(m^2·d)) (Smith and Demaster, 1996; Hung et al., 2013), most of the OC loadings in the neritic zone (e.g., <0.4 mg OC/m^2 in the ECS inner shelf and the Amazon) are even lower than those of the bathyal zone (e.g., ~0.5 mg OC/m^2 on average in the NW Atlantic slope (POC flux ~1.8 mg OC/(m^2·d)) and the Gulf of Lyon (POC flux ~1.0 mg OC/(m^2·d))) (Fig.6) (Conte et al., 2001; Peterson et al., 2005) (Fig.3). Similarly, OC loading within the Yap Trench decreased more than 17% with increasing water depth, from 0.10±0.03 mg OC/m^2 at 4 435 m depth to 0.05±0.04 mg OC/m^2 at 6 775 m depth (Table 1). This decrease with depth is most likely a result of frequent sediment collapse caused by submarine earthquakes, which also induce resuspension of unconsolidated submarine plain and trench sediments and subsequent long-distance lateral transport of SOC (Oguri et al., 2013; Ichino et al., 2015; Bao et al., 2018). A previous study demonstrated that approximately 24%–56% of settling POC at 8681 m depth in the Japan Trench may have come from resuspended surface sediments in adjacent trench slopes and that the contribution of resuspended OC to the total POC pool increases with water depth (Nakatsuka et al., 1997, 2000). Simultaneously, although due to the funneling effect in the V-shaped structure trench (Fig.1a) (Glud et al., 2013; Li et al., 2018), the average surface OC% in the Yap Trench (~0.5%) is higher than those in the normal deep open seas (e.g., ~0.27% in the central Indian Basin, ~0.35% in the NE Pacific Ocean, ~0.3% in the equatorial Pacific Ocean) and even comparable with those in the neritic region (e.g., ~0.5% in Amazon-Guiana mud belt, ~0.47% in the inner continental shelf of ECS and ~0.6% in the Washington slope) (Mayer, 1994a; Aller and Blair, 2006; Zhang et al., 2008; Li et al., 2014). However, the DO-enriched water interface (4.4–9.9 mg/L) (Li et al., 2018), increasing benthic microorganism abundance and OC remineralization rate (estimated by the benthic oxygen consumption rate) with increasing water depth in the hadal zone (Glud et al., 2013; Wu et al., 2018b) lead to significantly lower average OC loading in sedimentary cores compared to average marine environments (Figs.5 & 6).

To track the effects of the physical structure of sedimentary particles on OC loadings, trends in the variation of sediment SSA with water depth, OC% and OC loadings were also compared. In most marine regimes, SSA values varies from ~10 to ~60 m^2/g (Fig.4a & b), from the range of detrital minerals (e.g., feldspar, olivine and pyroxene, 0.02–1.8 m^2/g) (Nielsen and Fisk, 2008, 2010) to that of phytoplankton debris (e.g., diatoms, 20–200 m^2/g) (Dixit et al., 2001; Loucaides et al., 2010, 2012). The SSA values showed an increasing trend with increasing water depth (Fig.4c), indicating an increasing contribution of biogenic debris to sediments. Although SSA values are positively correlated with OC% (Fig.4a & b), SSA values are negatively correlated with OC loadings (Fig.4d), which is probably due to increasing SSA values and decreasing OC% with greater water depth (Figs.4c & 5). In addition, a positive intercept of approximately 0.03% on OC% in the plot of SSA versus OC% for the Yap Trench may indicate that some of the SOC did not originate from adsorption, such as the addition of rock OC or plant-derived OC (Fig.5) (Keil et al., 1994; Bergamaschi et al., 1997; Vonk et al., 2012; Tesi et al., 2016). We conjecture that this part of OC can be mainly ascribed to OC from plant tissues rather than rock OC since sedimentary rock OC is mostly found in continental regions near the mouths of large rivers (Tesi et al., 2016). The fractional contribution of this OC to the total OC pool is approximately 12%, which is consistent with the end-member model calculation of the proportion of

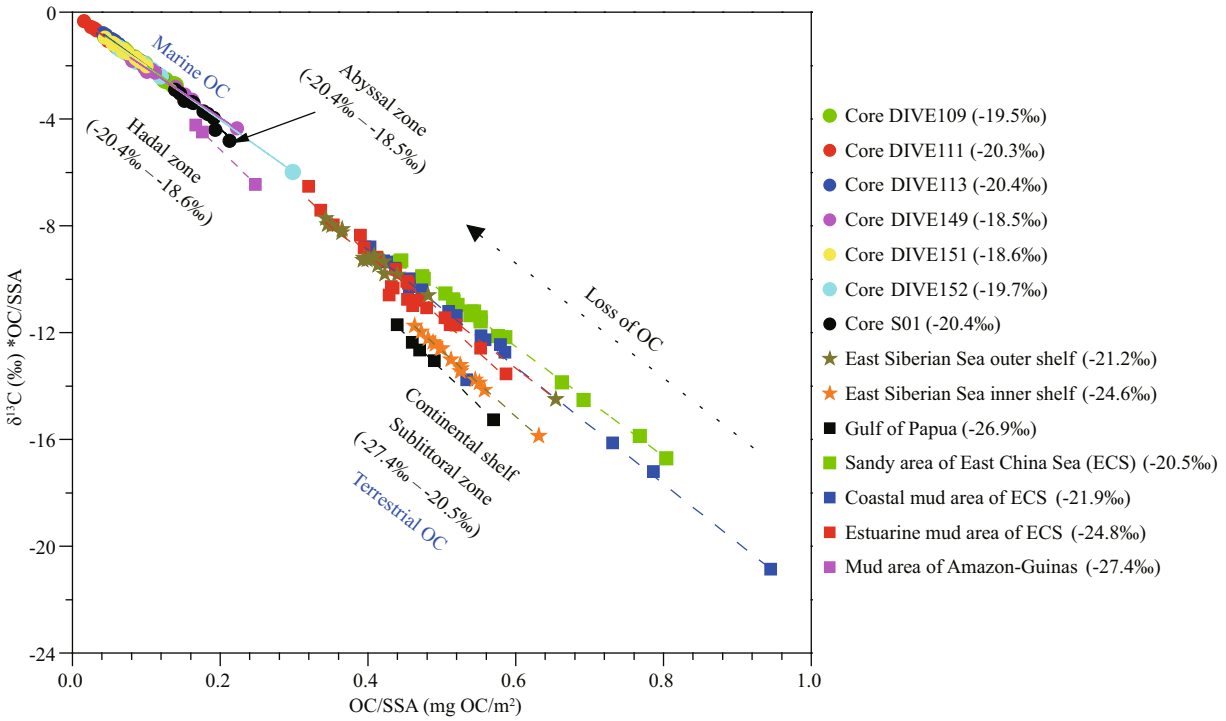

Fig.7 Relationships between OC loadings and bulk OC isotopic compositions in sediment cores from hadal, abyssal and neritic regions (Aller and Blair, 2006; Aller et al., 2008; Bröder et al., 2016; Tesi et al., 2016)

vascular plant-derived OC in Yap Trench SOC (8%±2%) (Wu et al., 2018a).

4.2 Sources of remineralized SOC and preservation of SOC

Because the ranges of SOC loadings have been seen as effective indicators of the net balances between OC supply and remineralization reactions (Aller and Blair, 2004; Blair and Aller, 2012; Yao et al., 2014), relationships between SOC loadings and bulk carbon isotope compositions have been used to identify sources of remineralized SOC (Blair and Aller, 2012; Wu et al., 2018b). As illustrated by previous studies, the loss of SOC (decrease of OC loading) is a progressive reaction, and by plotting product of $\delta^{13}C$ and the OC-loading vs. the OC loading in core sediments and employing linear fitting, the calculated geometric mean slopes of these regression lines can be taken to represent the characteristic $\delta^{13}C$ values of lost SOC ($\delta^{13}C_{lost\ SOC}$). As shown in Fig.7, $\delta^{13}C_{lost\ SOC}$ values are approximately -20.4‰– -18.6‰ within the Yap Trench, showing no significant spatial differences and indicating that the lost SOC pool is dominantly composed of marine OC ($\delta^{13}C$ value around -20.0‰±3.0‰, Li et al., 2012), with an additional small fraction of terrestrial OC ($\delta^{13}C$ value around 25.2‰±3.9‰, Alin et al., 2008; Francisquini et al., 2014). This result is consistent with the conclusion that the OC compositions are similar in the SOC pool down through the trench, despite different OC% (Wu et al., 2018a). Additionally, phytoplankton-derived OC has been shown to dominate SOC pools in the hadal trench (e.g., the Mariana Trench, Luo et al., 2017), the small proportion of terrestrial OC in the SOC pool (Wu et al., 2018a, b) and the preferential consumption of ^{13}C- and nitrogen-enriched organic matter by heterotrophic microbes also lead to the selective utilization of marine OC (Nakatsuka et al., 1997; Wu et al., 2018b). However, although marine phytoplankton production is higher in the continental inner shelf compared with open ocean environments (Falkowski et al., 1998), the $\delta^{13}C_{lost\ SOC}$ value in the sublittoral zone (e.g., continental inner shelf, -27.4‰ to -20.5‰) was much lower than those of the Yap Trench and abyssal zones (-20.4‰ to -18.5‰) (Fig.7). We speculate that the major reasons for this difference are the relative contribution of fresh terrestrial OC to the SOC pool and the possible formation of organometallic chelates. Specifically, the addition of significant riverine terrestrial material inputs in continental marginal seas lead to higher fractional contributions of terrestrial OC to the SOC pool observed in sublittoral zones (e.g., ~65% in ECS inner shelf) compared to hadal trenches (e.g., 11%–30% in Yap Trench) (Yao et al., 2015; Wu et al., 2018a, b). Meanwhile, due to the coarser grain size

and weaker binding ability of terrestrial OC to iron oxide minerals than those of marine OC, most of the iron-chelated OC exhibits heavier ^{13}C signals (enriched in proteins and carbohydrates with more nitrogen and/or oxygen functionalities), and thus most of remineralized OC is ^{13}C depleted (Müller and Suess, 1980; Hartnett et al., 1998; Zonneveld et al., 2010; Lalonde et al., 2012; Zhao et al., 2016). For example, the percentage of marine OC chelated by active iron oxide relative to the total SOC pool has been shown to be as high as 21% in the south Yellow Sea sediments (Tao et al., 2017).

Compared with average marine environments, OC preservation capacities in the Yap Trench were significantly lower (Fig.3b). First, the preservation of SOC is positively well correlated with the sediment accumulation rate, especially for oxygenated systems receiving predominately marine OC (Müller and Suess, 1980; Hartnett et al., 1998; Blair and Aller, 2012). In the hadal trench, the oxygen-enriched sediment-water interface (DO ~4.4–9.9 mg/L) and deep dissolved oxygen penetration depth in the sediments (~tens of centimeters) provide an ideal microenvironment for aerobic respiration by benthic microorganisms (Zhu et al., 2011; Jamieson, 2015; Li et al., 2018). Higher oxygen consumption rates and degradation rates of SOC have been reported in the deeper regions of the hadal zone than in other ocean environments (Glud et al., 2013; Wu et al., 2018b). In continental marginal seas, the development of oxygen-depleted and hypoxic regions (DO <4 mg/L) and higher sediment accumulation rates promote the preservation of SOC by controlling redox conditions and changing the remineralization pathways (Müller and Suess, 1980; Aller et al., 1985; Henrichs and Reeburgh, 1987). In support of this hypothesis, anaerobic respiration has been shown to be much less efficient in the degradation of SOC than aerobic respiration (Henrichs and Reeburgh, 1987; Zhu et al., 2011). Second, remarkable riverine inputs of terrigenous ferric oxide minerals into continental marginal seas leads to active inner-sphere complexation between OC and iron oxides. The formation of Fe-OC aggregates substantially shelters OC and protect OC from reacting with catabolic enzymes and transfers a large amount of OC to sedimentary sink (i.e. the "iron gate" effect) (Zhao et al., 2016; Barber et al., 2017; Wang et al., 2017).

Although a significant funneling effect for the trapping of SOC occurs in the hadal zone (Glud et al., 2013; Luo et al., 2017), our results indicate that most of the SOC is quickly consumed in the upper tens of centimeters of deposits, and only approximately 30%±11% of the POC settling onto the surface sediment of the hadal zone is ultimately buried (Fig.3b). In addition, if the regional primary production rate (~82 g OC/(m^2·a)) (Jamieson, 2015) and the accumulation rate of surface SOC in the Yap Trench (~0.18 g OC/(m^2·a)) (Wu et al., 2018b) are combined, the fraction of OC ultimately preserved in the Yap Trench would be only approximately 0.066% of the primary production, which was only 22% of global ocean averages (~0.3%, Amon, 2016), indicating weak burial of SOC in hadal environments.

5 CONCLUSION

In this study, we obtained insight into the pattern of variations in OC loadings in sediments under different marine regimes. Both pre-depositional processes, such as the water depth and oxygen exposure time during the particle settling, and post-depositional process, such as reworking of sediments in hydrodynamic environments are found to be important in controlling the OC loading distribution pattern. The average OC loadings in sediment cores from various marine regimes exhibited decreasing trends with greater water depth, and a OC/SSA ratio of 0.2 mg OC/m^2 is a good indicator to distinguish oxic deep sea regions from suboxic energetic deltaic areas. Regression analysis between OC loading and bulk carbon isotope compositions reveal that sources of remineralized SOC changed from marine OC-dominated SOC in abyssal and hadal zones to terrestrial OC-dominated SOC in the sublittoral zone. This result is likely due to the relative proportions of terrestrial and marine OC in different marine environments and the probable "iron gate" effect. For SOC preservation capacities of sediments in different marine environments, only approximately 30% of deposited SOC is likely to finally buried in hadal trenches, which is much lower than in other marine environments. The buried SOC in the Yap Trench was only ~0.066% of primary production-derived OC and much lower than the global ocean average (~0.3%). This study demonstrates that the hadal trench has the lowest OC loading and preservation capacity of SOC among the different marine environments investigated, although a significant funneling effect is also found to occur there. The outcomes of this study will extend our knowledge of the final fate of SOC under different marine environments.

6 DATA AVAILABILITY STATEMENT

The authors declare that the data supporting the findings of this study are available within the article and its electronic supplementary files. And the data in this study are also available from the authors upon reasonable request.

7 ACKNOWLEDGMENT

We are grateful to the crews of the R/V *Xiangyanghong 10*, LU Bo, LI Zhongqiao, ZHU Qiuhong, and GUO Xiaoze in the Second Institute of Oceanography (MNR), and PENG Yao, WU Dan and YE Jun of the Ocean University of China for their help in sampling and technical support with analyses.

References

Alin S R, Aalto R, Goni M A, Richey J E, Dietrich W E. 2008. Biogeochemical characterization of carbon sources in the Strickland and Fly rivers, Papua New Guinea. *Journal of Geophysical Research*: *Earth Surface*, **113**: F01S05, https://doi.org/10.1029/2006JF000625.

Aller R C. 1998. Mobile deltaic and continental shelf muds as suboxic, fluidized bed reactors. *Marine Chemistry*, **61**(3-4): 143-155.

Aller R C, Blair N E. 2004. Early diagenetic remineralization of sedimentary organic C in the Gulf of Papua deltaic complex (Papua New Guinea): net loss of terrestrial C and diagenetic fractionation of C isotopes. *Geochimica et Cosmochimica Acta*, **68**(8): 1 815-1 825.

Aller R C, Blair N E. 2006. Carbon remineralization in the Amazon-Guianas tropical mobile mudbelt: a sedimentary incinerator. *Continental Shelf Research*, **26**(17-18): 2 241-2 259.

Aller R C, Blair N E, Brunskill G J. 2008. Early diagenetic cycling, incineration, and burial of sedimentary organic carbon in the central Gulf of Papua (Papua New Guinea). *Journal of Geophysical Research*: *Earth Surface*, **113**(F1): F01S09, https://doi.org/10.1029/2006JF000689.

Aller R C, Mackin J E, Ullman W J, Wang C H, Tsai S M, Jin J C, Sui Y N, Hong J Z. 1985. Early chemical diagenesis, sediment-water solute exchange, and storage of reactive organic matter near the mouth of the Changjiang, East China Sea. *Continental Shelf Research*, **4**(1-2): 227-251.

Aller R C, Madrid V, Chistoserdov A, Aller J Y, Heilbrun C. 2010. Unsteady diagenetic processes and sulfur biogeochemistry in tropical deltaic muds: implications for oceanic isotope cycles and the sedimentary record. *Geochimica et Cosmochimica Acta*, **74**(16): 4 671-4 692.

Amon R M W. 2016. Ocean dissolved organics matter. *Nature Geoscience*, **9**(12): 864-865.

Bao R, Strasser M, McNichol A P, Haghipour N, Mclntyre C, Wefer G, Eglinton T I. 2018. Tectonically-triggered sediment and carbon export to the hadal zone. *Nature Communications*, **9**(1): 121.

Barber A, Brandes J, Leri A, Lalonde K, Balind K, Wirick S, Wang J, Gélinas Y. 2017. Preservation of organic matter in marine sediments by inner-sphere interactions with reactive iron. *Scientific Reports*, **7**(1): 366.

Bergamaschi B A, Tsamakis E, Keil R G, Eglinton T I, Montluçon D B, Hedges J I. 1997. The effect of grain size and surface area on organic matter, lignin and carbohydrate concentration, and molecular compositions in Peru Margin sediments. *Geochimica et Cosmochimica Acta*, **61**(6): 1 247-1 260.

Blair N E, Aller R C. 2012. The fate of terrestrial organic carbon in the marine environment. *Annual Review of Marine Science*, **4**(1): 401-423.

Bröder L, Tesi T, Andersson A, Eglinton T I, Semiletov I P, Dudarev O V, Roos P, Gustafsson Ö. 2016. Historical records of organic matter supply and degradation status in the East Siberian Sea. *Organic Geochemistry*, **91**: 16-30.

Chen J F, Jin H Y, Li H L, Zhang H S, Ji Z Q, Zhuang Y P, Bai Y C. 2015. Carbon sink mechanism and processes in the Arctic Ocean under arctic rapid change. *Chinese Science Bulletin*, **60**(35): 3 406-3 416.

Chen J F, Zhang H S, Jin H Y, Jin M M, Liu Z L. 2004. Accumulation of sedimentary organic carbon in the arctic shelves and its significance on global carbon budget. *Chinese Journal of Polar Research*, **16**(3): 193-201. (in Chinese with English abstract)

Clift P, Vannucchi P. 2004. Controls on tectonic accretion versus erosion in subduction zones: Implications for the origin and recycling of the continental crust. *Reviews of Geophysics*, **42**(2): RG2001, https://doi.org/10.1029/2003RG000127.

Conte M H, Ralph N, Ross E H. 2001. Seasonal and interannual variability in deep ocean particle fluxes at the Oceanic Flux Program (OFP)/Bermuda Atlantic Time Series (BATS) site in the western Sargasso Sea near Bermuda. *Deep Sea Research Part II*: *Topical Studies in Oceanography*, **48**(8-9): 1 471-1 505.

Danovaro R, Croce N D, Dell'Anno A, Pusceddu A. 2003. A depocenter of organic matter at 7800 m depth in the SE Pacific Ocean. *Deep Sea Research Part I*: *Oceanographic Research Papers*, **50**(12): 1 411-1 420.

Dixit S, van Cappellen P, van Bennekom A J. 2001. Processes controlling solubility of biogenic silica and pore water build-up of silicic acid in marine sediments. *Marine Chemistry*, **73**(3-4): 333-352.

Falkowski P G, Barber R T, Smetacek V. 1998. Biogeochemical controls and feedbacks on ocean primary production. *Science*, **281**(5374): 200-206.

Francisquini M I, Lima C M, Pessenda L C R, Rossetti D F, França M C, Cohen M C L. 2014. Relation between carbon isotopes of plants and soils on Marajó Island, a large tropical island: implications for interpretation of modern and past vegetation dynamics in the Amazon region. *Palaeogeography*, *Palaeoclimatology*, *Palaeoecology*, **415**: 91-104.

Fujio S, Yanagimoto D, Taira K. 2000. Deep current structure above the Izu-Ogasawara Trench. *Journal of Geophysical*

Research: *Oceans*, **105**(C3): 6 377-6 386.

Fujiwara T, Tamura C, Nishizawa A, Fujioka K, Kobayashi K, Iwabuchi Y. 2000. Morphology and tectonics of the Yap Trench. *Marine Geophysical Researches*, **21**(1-2): 69-86.

Glud R N, Wenzhöfer F, Middelboe M, Oguri K, Turnewitsch R, Canfield D E, Kitazato H. 2013. High rates of microbial carbon turnover in sediments in the deepest oceanic trench on Earth. *Nature Geoscience*, **6**(4): 284-288.

Goñi M A, O'Connor A E, Kuzyk Z Z, Yunker M B, Gobeil C, Macdonald R W. 2013. Distribution and sources of organic matter in surface marine sediments across the North American Arctic margin. *Journal of Geophysical Research*: *Oceans*, **118**(9): 4 017-4 035.

Hallock Z R, Teague W J. 1996. Evidence for a North Pacific deep western boundary current. *Journal of Geophysical Research*: *Oceans*, **101**(C3): 6 617-6 624.

Hartnett H E, Keil R G, Hedges J I, Devol A H. 1998. Influence of oxygen exposure time on organic carbon preservation in continental margin sediments. *Nature*, **391**(6667): 572-575.

Henrichs S M, Reeburgh W S. 1987. Anaerobic mineralization of marine sediment organic matter: rates and the role of anaerobic processes in the oceanic carbon economy. *Geomicrobiology Journal*, **5**(3-4): 191-237.

Honjo S, Manganini S J, Krishfield R A, Francois R. 2008. Particulate organic carbon fluxes to the ocean interior and factors controlling the biological pump: a synthesis of global sediment trap programs since 1983. *Progress in Oceanography*, **76**(3): 217-285.

Hung C C, Tseng C W, Gong G C, Chen K S, Chen M H, Hsu S C. 2013. Fluxes of particulate organic carbon in the East China Sea in summer. *Biogeosciences*, **10**(10): 6 469-6 484.

Ichino M C, Clark M R, Drazen J C, Jamieson A, Jones D O B, Martin A P, Rowden A A, Shank T M, Yancey P H, Ruhl H A. 2015. The distribution of benthic biomass in hadal trenches: a modelling approach to investigate the effect of vertical and lateral organic matter transport to the seafloor. *Deep Sea Research Part I*: *Oceanographic Research Papers*, **100**: 21-33.

Jamieson A. 2015. The Hadal Zone: Life in the Deepest Oceans. England: Cambridge University Press.

Jamieson A J, Fujii T. 2011. Trench connection. *Biology Letters*, **7**(5): 641-643.

Keil R G, Mayer L M, Quay P D, Richey J E, Hedges J I. 1997b. Loss of organic matter from riverine particles in deltas. *Geochimica et Cosmochimica Acta*, **61**(7): 1 507-1 511.

Keil R G, Tsamakis E, Fuh C B, Giddings J C, Hedges J I. 1994. Mineralogical and textural controls on the organic composition of coastal marine sediments: hydrodynamic separation using SPLITT-fractionation. *Geochimica et Cosmochimica Acta*, **58**(2): 879-893.

Keil R G, Tsamakis E, Wolf N, Hedges J I, Goñi M. 1997a. 33. Relationships between organic carbon preservation and mineral surface area in Amazon fan sediments (Holes 932A and 942A). *In*: Flood R D, Piper D J W, Klaus A, Peterson L C eds. Proceedings of the Ocean Drilling Program, Scientific Results, **155**: 531-538.

Lalonde K, Mucci A, Ouellet A, Gélinas Y. 2012. Preservation of organic matter in sediments promoted by iron. *Nature*, **483**(7388): 198-200.

Lasaga A C, Berner R A, Garrels R M. 1985. An improved geochemical model of atmospheric CO_2 fluctuations over the past 100 million years. *In*: The Carbon Cycle and Atmospheric CO_2: Natural Variations Archean to Present, Volume 32. American Geophysical Union, 397-411, https://doi.org/10.1029/GM032p0397.

Li D, Yao P, Bianchi T S, Zhang T T, Zhao B, Pan H H, Wang J P, Yu Z G. 2014. Organic carbon cycling in sediments of the Changjiang Estuary and adjacent shelf: implication for the influence of Three Gorges Dam. *Journal of Marine Systems*, **139**: 409-419.

Li D, Zhao J, Liu C G, Sun C J, Chen J F, Pan J M, Yang Z, Wang K, Han Z B, Yu P S. 2018. Advances of living environment characteristics and biogeochemical processes in the hadal zone. *Earth Science*, (S2): 162-178. (in Chinese with English abstract)

Li X X, Bianchi T S, Allison M A, Chapman P, Mitra S, Zhang Z R, Yang G P, Yu Z G. 2012. Composition, abundance and age of total organic carbon in surface sediments from the inner shelf of the East China Sea. *Marine Chemistry*, **145-147**: 37-52.

Li Z Q, Wang X Y, Jin H Y, Ji Z Q, Bai Y C, Chen J F. 2017. Variations in organic carbon loading of surface sediments from the shelf to the slope of the Chukchi Sea, Arctic Ocean. *Acta Oceanologica Sinica*, **36**(8): 131-136.

Longhurst A, Sathyendranath S, Platt T, Caverhill C. 1995. An estimate of global primary production in the ocean from satellite radiometer data. *Journal of Plankton Research*, **17**(6): 1 245-1 271.

Loucaides S, Behrends T, van Cappellen P. 2010. Reactivity of biogenic silica: surface versus bulk charge density. *Geochimica et Cosmochimica Acta*, **74**(2): 517-530.

Loucaides S, van Cappellen P, Roubeix V, Moriceau B, Ragueneau O. 2012. Controls on the recycling and preservation of biogenic silica from biomineralization to burial. *Silicon*, **4**(1): 7-22.

Luo M, Gieskes J, Chen L Y, Shi X F, Chen D F. 2017. Provenances, distribution, and accumulation of organic matter in the southern Mariana Trench rim and slope: implication for carbon cycle and burial in hadal trenches. *Marine Geology*, **386**: 98-106.

Lutz M J, Caldeira K, Dunbar R B, Behrenfeld M J. 2007. Seasonal rhythms of net primary production and particulate organic carbon flux to depth describe the efficiency of biological pump in the global ocean. *Journal of Geophysical Research*: *Oceans*, **112**(C10): C10011, https://doi.org/10.1029/2006JC003706.

Mayer L M. 1994a. Relationships between mineral surfaces and organic carbon concentrations in soils and sediments. *Chemical Geology*, **114**(3-4): 347-363.

Mayer L M. 1994b. Surface area control of organic carbon accumulation in continental shelf sediments. *Geochimica et Cosmochimica Acta*, **58**(4):1 271-1 284.

Mayer L M. 1995. Sedimentary organic matter preservation: an assessment and speculative synthesis—a comment. *Marine Chemistry*, **49**(2-3): 123-126.

Müller P J, Suess E. 1980. Productivity, sedimentation rate, and sedimentary organic matter in the oceans—I. organic carbon preservation. *Deep Sea Research Part A. Oceanographic Research Papers*, **26**(12): 1 347-1 362.

Nakatsuka T, Handa N, Harada N, Sugimoto T, Lmaizumi S. 1997. Origin and decomposition of sinking particulate organic matter in the deep water column inferred from the vertical distributions of its $\delta^{15}N$, $\delta^{13}C$ and $\delta^{14}C$. *Deep Sea Research Part I*: *Oceanographic Research Papers*, **44**(12): 1 957-1 979.

Nakatsuka T, Hosokawa A, Handa N, Matsumoto E, Masuzawa T. 2000. ^{14}C budget of sinking particulate organic matter in the Japan Trench: a new approach to estimate the contribution from resuspended particles in deep water column. *In*: Handa N, Tanoue E, Hama T eds. Dynamics and Characterization of Marine Organic Matter. Ocean Sciences Research. Dordrecht: Springer, **2**: 169-186.

Nath B N, Khadge N H, Nabar S, Kumar C R, Ingole B S, Valsangkar A B, Sharma R, Srinivas K. 2012. Monitoring the sedimentary carbon in an artificially disturbed deep-sea sedimentary environment. *Environmental Monitoring and Assessment*, **184**(5): 2 829-2 844.

Nielsen M E, Fisk M R. 2008. Data report: specific surface area and physical properties of subsurface basalt samples from the east flank Juan de Fuca Ridge. *In*: Proceedings of the Integrated Ocean Drilling Program, Volume 301.

Nielsen M E, Fisk M R. 2010. Surface area measurements of marine basalts: implications for the subseafloor microbial biomass. *Geophysical Research Letters*, **37**(15): L15604, https://doi.org/10.1029/2010GL044074 .

Nozaki Y, Ohta Y. 1993. Rapid and frequent turbidite accumulation in the bottom of Izu-Ogasawara Trench: chemical and radiochemical evidence. *Earth and Planetary Science Letters*, **120**(3-4): 345-360.

Nunoura T, Takaki Y, Hirai M, Shimamura S, Makabe A, Koide O, Kikuchi T, Miyazaki J, Koba K, Yoshida N, Sunamura M, Takai K. 2015. Hadal biosphere: insight into the microbial ecosystem in the deepest ocean on Earth. *Proceedings of the National Academy of Sciences of the United States of America*, **112**(11): E1 230-E1 236.

Oguri K, Kawamura K, Sakaguchi A, Toyofuku T, Kasaya T, Murayama M, Fujikura K, Glud R N, Kitazato H. 2013. Hadal disturbance in the Japan Trench induced by the 2011 Tohoku-Oki Earthquake. *Scientific Reports*, **3**: 1 915.

Peterson M L, Wakeham S G, Lee C, Askea M A, Miquel J C. 2005. Novel techniques for collection of sinking particles in the ocean and determining their settling rates. *Limnology and Oceanography*: *Methods*, **3**(12): 520-532.

Smith W O Jr, Demaster D J. 1996. Phytoplankton biomass and productivity in the Amazon River plume: correlation with seasonal river discharge. *Continental Shelf Research*, **16**(3): 291-319.

Taira K, Kitagawa S, Yamashiro T, Yanagimoto D. 2004. Deep and bottom currents in the challenger deep, mariana trench, measured with super-deep current meters. *Journal of Oceanography*, **60**(6): 919-926.

Tao J, Ma W W, Li W J, Li T, Zhu M X. 2017. Organic carbon preservation by reactive iron oxides in South Yellow Sea sediments. *Haiyang Xuebao*, **39**(8): 16-24. (in Chinese with English abstract)

Tesi T, Semiletov I, Dudarev O, Andersson A, Gustafsson Ö. 2016. Matrix association effects on hydrodynamic sorting and degradation of terrestrial organic matter during cross-shelf transport in the Laptev and East Siberian shelf seas. *Journal of Geophysical Research*: *Biogeosciences*, **121**(6): 731-752.

Vonk J E, Giosan L, Blusztajn J, Montlucon D, Graf Pannatier E, McIntyre C, Wacker L, Macdonald R W, Yunker M B, Eglinton T I. 2015. Spatial variations in geochemical characteristics of the modern Mackenzie Delta sedimentary system. *Geochimica et Cosmochimica Acta*, **171**: 100-120.

Vonk J E, Sánchez-García L, van Dongen B E, Alling V, Kosmach D, Charkin A, Semiletov I P, Dudarev O V, Shakhova N, Roos P, Eglinton T I, Andersson A, Gustafsson Ö. 2012. Activation of old carbon by erosion of coastal and subsea permafrost in Arctic Siberia. *Nature*, **489**(7414): 137-140.

Wang Y Y, Wang H, He J S, Feng X J. 2017. Iron-mediated soil carbon response to water-table decline in an alpine wetland. *Nature Communications*, **8**: 15 972.

Wu B, Li D, Zhao J, Liu C G, Sun C J, Chen J F, Pan J M, Han Z B, Hu J. 2018a. Influence of sedimentary environment on composition and distribution of sediments in the Yap Trench. *Haiyang Xuebao*, **40**(10): 167-179. (in Chinese with English abstract)

Wu B, Li D, Zhao J, Liu C G, Sun C J, Chen J F, Pan J M, Han Z B, Hu J. 2018b. Vertical distribution of sedimentary organic carbon in the yap trench and its implications. *China Environmental Science*, **38**(9): 3 502-3 511. (in Chinese with English abstract)

Yao P, Yu Z G, Bianchi T S, Guo Z G, Zhao M X, Knappy C S, Keely B J, Zhao B, Zhang T T, Pan H H, Wang J P, Li D. 2015. A multiproxy analysis of sedimentary organic carbon in the Changjiang Estuary and adjacent shelf. *Journal of Geophysical Research*: *Biogeosciences*, **120**: 1 407-1 429.

Yao P, Zhao B, Bianchi T S, Guo Z G, Zhao M X, Li D, Pan H H, Wang J P, Zhang T T, Yu Z G. 2014. Remineralization of sedimentary organic carbon in mud deposits of the Changjiang Estuary and adjacent shelf: implications for carbon preservation and authigenic mineral formation. *Continental Shelf Research*, **91**: 1-11.

Yue X A, Yan Y X, Ding H B, Sun C J, Yang G P. 2018. Biological geochemical characteristics of the sediments in the yap trench and its oceanographic significance. *Periodical of Ocean University of China*, **48**(3): 88-96. (in Chinese with English abstract)

Zhang H S, Yu P S, Ni J Y, Wu G H, Sun W P, Lu B. 2008. Geochemical contrast of the physical properties, the

source characters and the depositional environment of the organic matter from the different strata of the equatorial Pacific area. *Acta Oceanologica Sinica*, **30**(6): 60-68. (in Chinese with English abstract)

Zhao B, Yao P, Yu Z G. 2016. The effect of organic carbon-iron oxide association on the preservation of sedimentary organic carbon in marine environments. *Advances in Earth Science*, **31**(11): 1 151-1 158. (in Chinese with English abstract)

Zhu M X, Shi X N, Yang G P, Li T, Lv R Y. 2011. Relative contributions of various early diagenetic pathways to mineralization of organic matter in marine sediments: an overview. *Advances in Earth Science*, **26**(4): 355-364. (in Chinese with English abstract)

Zonneveld K A F, Versteegh G J M, Kasten S, Eglinton T I, Emeis K C, Koch B P, de Lange G J, de Leeuw J W, Middelburg J J, Mollenhauer G, Prahl F G, Rethemeyer J, Wakeham S G. 2010. Selective preservation of organic matter in marine environments; processes and impact on the sedimentary record. *Biogeoscience*s, **7**(2): 483-511.

Electronic supplementary material

Supplementary material (Supplementary Tables S1–S2) is available in the online version of this article at https://doi.org/10.1007/s00343-019-8365-9.